

Spin-torque ferromagnetic resonance measurements of damping in nanomagnets

G. D. Fuchs,^{a)} J. C. Sankey, V. S. Pribiag, L. Qian, P. M. Braganca, A. G. F. Garcia, E. M. Ryan, Zhi-Pan Li, O. Ozatay, D. C. Ralph, and R. A. Buhrman
Cornell University, Ithaca, New York 14853–2501

(Received 21 March 2007; accepted 10 July 2007; published online 7 August 2007)

The authors directly measure the magnetic damping parameter α in thin-film CoFeB and Permalloy (Py) nanomagnets at room temperature using a recently developed ferromagnetic resonance technique where the precessional mode of an individual nanomagnet can be excited by microwave-frequency spin-transfer torque and detected by the giant magnetoresistance effect. The authors obtain $\alpha_{\text{CoFeB}}=0.014\pm 0.003$ and $\alpha_{\text{Py}}=0.010\pm 0.002$, values comparable to measurements for extended thin films, establishing that patterned nanomagnets can exhibit magnetic damping that is consistent with that of unpatterned bulk material. © 2007 American Institute of Physics.

[DOI: [10.1063/1.2768000](https://doi.org/10.1063/1.2768000)]

Dissipation in nanoscale magnetic systems is of widespread fundamental interest due to its role in the magnetization dynamics of spatially confined magnetic elements.¹ In addition, understanding and controlling magnetic damping is important for minimizing the switching current in proposed future generations of magnetic memory switched by spin torque² (ST) and for counteracting ST-excited magnetic noise, which may limit the areal density in future generations of hard drives that use giant magnetoresistance (GMR) read heads.³ Magnetic damping is usually characterized by the phenomenological damping parameter α , which can have both intrinsic and extrinsic contributions. The latter includes surface effects, which may be particularly important in patterned magnetic nanostructures. Furthermore, in multilayer structures, the pumping of spins from a precessing magnetic moment can also cause additional damping,^{4,5} an effect which may depend on the amplitude of the excitation.⁶

Although conventional damping measurement techniques cannot be readily applied to individual nanoscale structures, experiments that employ spin-transfer torque to control magnetic dynamics can measure damping in nanomagnets via several approaches. In previous work, time-domain measurements of coherent relaxation oscillations of a Ni₈₁Fe₁₉ (Py) layer in a nanopillar spin valve device that was excited by spin torque from a short current pulse gave $\alpha=0.025$ at 40 K.⁷ Macrospin modeling⁸ of short-pulse ST-switching experiments has also yielded self-consistent results for the damping and spin-transfer efficiency over a broad range of experimental parameters.^{9,10} These fits gave values of α for Py nanomagnets at room temperature (RT) of 0.030–0.035, which are much larger than those obtained from conventional damping measurements on extended thin films^{11–13} (0.006–0.012). An analysis of pulse-switching measurements made at low temperature (LT) yielded even higher values,¹⁰ $\alpha\geq 0.05$. While a LT increase in damping can be attributed to the presence of an adventitious oxide around the perimeter of the nanomagnet that is cooled below the oxide's antiferromagnetic blocking temperature, the large RT values of α cannot readily be ascribed to either a native oxide or to spin pumping. This suggests either that α is larger at RT in nano-

pillar devices due to some additional effect, or that although macrospin modeling qualitatively and self-consistently describes the basics of ST switching^{8,14,15} it is not sufficiently approximate in describing the large-angle magnetization dynamics involved in ST switching to always yield accurate quantitative results.

We have now been able to examine this question by using spin-transfer-driven ferromagnetic resonance^{16–19} (ST-FMR) to directly measure RT small-angle precessional damping in spin valve nanopillars in the same low-field, hysteric regime employed in ST switching. We have determined the magnetic damping in both Py/Cu/Py and CoFeB/Cu/CoFeB devices and find $\alpha=0.010\pm 0.002$ and 0.014 ± 0.003 , respectively. The results demonstrate that the nanofabrication processes used to form magnetic nanopillars do not necessarily increase ferromagnetic damping, and thus indicate that the larger values of effective damping determined previously by the macrospin modeling of RT ST switching are due to the limitations of the macrospin approximation in describing the magnetic reversal process for these nanopillar devices.

We studied two types of magnetic multilayers (in nm): Ta 4/Cu 22/Ta 5/Cu 22/Ta 20/CoFeB 20/Cu 6/CoFeB 3.5/Cu 5/Pt 30 and Py 4/Cu 120/Py 20/Cu 12/Py 5.5/Cu 20/Pt 30. We will refer to the thicker magnetic layer in each device as the “fixed layer” and the thinner layer as the “free layer.” All films were deposited on thermally oxidized silicon wafers via dc magnetron sputtering at room temperature in a vacuum system with a base pressure of 3×10^{-8} torr. CoFeB was sputtered from an alloy target with atomic ratios of 60/20/20 and had a RT magnetization ($4\pi M$) of 14.8 kOe, while the Py had $4\pi M=7.0$ kOe. These multilayers were then patterned using electron-beam lithography and ion milling to form nanopillar spin valve structures, with approximately elliptical cross sections having the nominal dimensions of 50×110 nm for the CoFeB device and 55×130 nm² for the Py device. Our maximum processing temperature was 170 °C, so we expect that the CoFeB remained in the amorphous state after patterning.²⁰

Figure 1(a) shows a schematic of the ST-FMR measurement setup, which is similar to that used in Ref. 17. A microwave current I_{rf} , pulsed with an ~ 1.3 kHz repetition rate,

^{a)}Electronic mail: fuchs@cnsi.ucsb.edu

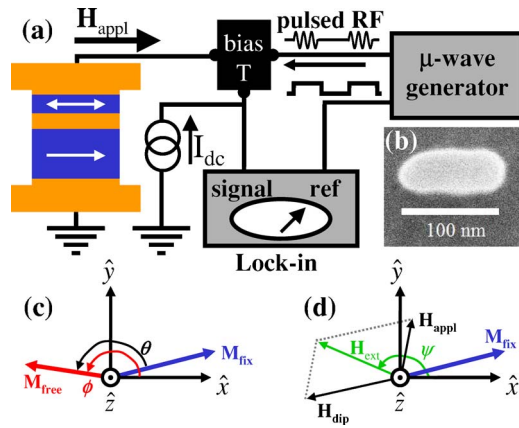


FIG. 1. (Color online) (a) Schematic diagram of the apparatus. (b) A top-view SEM image of an e-beam defined etch mask similar to the one used to form the CoFeB sample. (c) A diagram of magnetizations in our experiment. The thick arrows represent the approximate direction of M_{free} (red) and M_{fixed} (blue). The angle between them is the GMR angle θ . The angle ϕ is between M_{free} and the x axis. (d) A diagram of the fields in our experiment. H_{appl} marks the direction of the applied field. H_{ext} is the vector sum of H_{appl} and the dipolar field of the fixed layer (oriented 180° from M_{fixed}), oriented along an angle ψ in the film plane. Note that the angles and lengths in (c) and (d) are not exact, but instead have been exaggerated for clarity.

is applied perpendicular to the layers of the nanopillar to generate a microwave-frequency spin-transfer torque, which can excite precession in the magnetization of either the fixed or the free magnetic layers (or both) when the drive is resonant with a magnetic normal mode. We identify the origin of a particular mode by its frequency, which depends on the magnetic anisotropy of the specific layer, and confirm this identification by the mode's response to a direct current I_{dc} which can be applied simultaneously via a bias tee.

In order for the spin-transfer torque to be nonzero, the magnetizations of the fixed and free magnetic layers must be misaligned from either the strictly parallel or antiparallel configuration. In this experiment, we induce misalignment by applying an in-plane external field (H_{appl}) at a large angle with respect to the nanopillar easy axis¹⁶ [Fig. 1(b)]. Through the GMR effect, magnetic precession in the multilayer generates an ac resistance that mixes with I_{rf} to produce a rectified voltage, V_{mix} , which is detected with a lock-in amplifier. The misalignment angle is determined by the in-plane uniaxial anisotropies, H_k of the free and fixed layers for each sample. The value of H_k is dominated by the patterned elliptical shapes of the nanopillars since magneto-crystalline anisotropy is either small or absent in Py and amorphous CoFeB thin films. Using GMR measurements, we estimate that for the CoFeB sample $H_{k,\text{free}}=850$ Oe and $H_{k,\text{fix}}=700$ Oe, and for the Py sample $H_{k,\text{free}}=430$ Oe and $H_{k,\text{fix}}=440$ Oe.²¹

To measure the resonance linewidth, we apply constant microwave power to the sample and measure V_{mix} vs f at different values of I_{dc} . The effect of spin transfer from I_{dc} is to decrease the effective damping as I_{dc} is stepped to negative values, so that the resonant response to I_{rf} grows and the signal amplitude becomes larger as I_{dc} decreases toward the critical current. Figure 2(a) shows a representative ST-FMR peak for the CoFeB sample free layer, measured with $I_{\text{rf}}=0.18$ mA and $I_{\text{dc}}=-2.0$ mA, and with $H_{\text{appl}}=200$ Oe at an 80° angle with respect to the x axis. We estimate the GMR angle θ to be $\sim 163^\circ$ and that the free layer magnetization rotates to an angle ϕ of $\sim 177^\circ$ under the influence of H_{ext}

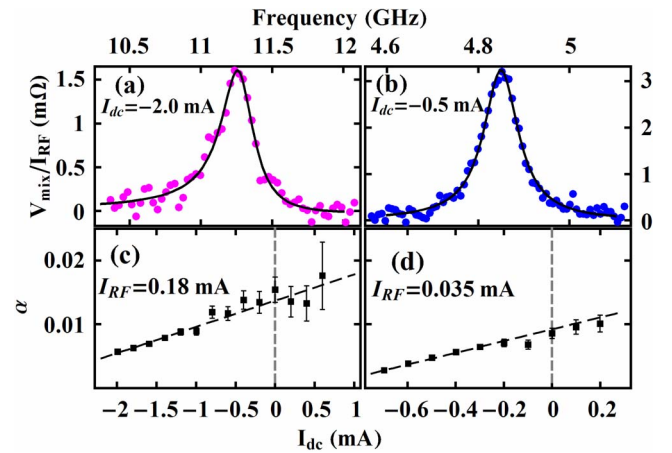


FIG. 2. (Color online) (a) ST-FMR data for the CoFeB sample taken at $H_{\text{appl}}=200$ Oe, $I_{\text{rf}}=0.18$ mA, and $I_{\text{dc}}=-2.0$ mA. The solid line is a Lorentzian fit. (b) Plot of the effective damping α vs I_{dc} for the CoFeB sample. The dashed line is a linear fit. (c) ST-FMR data for the Py sample taken at $H_{\text{appl}}=200$ Oe, $I_{\text{rf}}=-0.035$ mA, and $I_{\text{dc}}=-0.5$ mA. (d) Effective damping for the Py sample.

$=493$ Oe along an angle $\psi=172^\circ$ relative to the x axis [Figs. 1(c) and 1(d)]. H_{ext} is the vector sum of H_{appl} and the dipolar field of the fixed layer [Fig. 1(d)]. We have confirmed that the linewidth and line shape remain the same for smaller I_{rf} , indicating that we are operating in the linear-response regime. Based on the signal amplitude, the precessional angle for the $I_{\text{dc}}=2.0$ mA data is $\sim 6^\circ$, and for all other values of dc current that we report for the CoFeB sample, the precession angle is less than or equal to this value.

To determine the magnetic damping, we fit the ST-FMR line shapes to a combined symmetric and antisymmetric Lorentzian of the form

$$\frac{A}{1 + (f - f_o)^2 / \Delta_o^2} - \frac{B(f - f_o) / \Delta_o}{1 + (f - f_o)^2 / \Delta_o^2}. \quad (1)$$

An antisymmetric component of the ST-FMR line shape can arise when the spin-torque vector is not in a principal plane of the anisotropy tensor,^{18,19} or from contributions of an “effective field” component of spin torque perpendicular to the magnetizations of both magnetic layers.¹⁶ For our metal spin valve samples we find a small $|B/A|$ ratio between 0 and 0.07, which varies slightly among different samples, presumably due to anisotropy and shape variations. The damping α is related to Δ_o , the FMR half width, by¹⁹ $\alpha = \Delta_o / \Delta_k$, where $2\pi\Delta_k = \gamma 4\pi M(N'_y + N'_z) / 2$,

$$N'_y = (N_y - N_x)(\cos^2 \phi - \sin^2 \phi) + \cos(\psi - \phi)H_{\text{ext}} / (4\pi M), \quad (2)$$

$$N'_z = (N_z - N_x \cos^2 \phi - N_y \sin^2 \phi) + \cos(\psi - \phi)H_{\text{ext}} / (4\pi M), \quad (3)$$

where N_x, N_y, N_z are the demagnetization factors. Equations (2) and (3) describe the effective in-plane and out-of-plane anisotropy factors, respectively. For our samples, the determination of the damping from the FMR half width is dominated by the out-of-plane anisotropy since $N_x \approx N_y \approx 0$ and $N_z \approx 1$ in the thin-film limit. In determining the damping quantitatively, we use the demagnetization factors calculated from the sample geometry assuming that the free layers are elliptical cylinders.²² We find for the CoFeB free layer: N_x

$=0.034$, $N_y=0.091$, $N_z=0.876$, and for the Py free layer, $N_x=0.044$, $N_y=0.105$, $N_z=0.851$. These numbers are consistent with the observed FMR frequencies as well as with 4 K coercive fields in multiple samples with the same geometry.

Figure 2(c) shows α as a function of I_{dc} for the CoFeB free layer determined from this fitting procedure. We find that α depends linearly on I_{dc} as expected for the lowest-frequency free layer mode, because spin transfer from I_{dc} should modify the effective damping.²³ The regression line gives $\alpha=0.014\pm 0.003$ at $I_{dc}=0$. We estimate the error by propagating uncertainty in the determination of the anisotropies, the magnetization angles, as well as from fits to the data. In addition, when we perform damping measurements with an initial magnetization state misaligned from the parallel (rather than the antiparallel) configuration, we find the same value of α within the experimental accuracy.

We measured the Py sample at $H_{app1}=200$ Oe with at a 70° angle from the easy axis, which induces an $\sim 154^\circ$ GMR angle with $\phi\sim 172^\circ$, $\psi=158^\circ$, and $H_{ext}=245$ Oe. Figure 2(b) shows the resonant response with $I_{rf}=0.035$ mA and $I_{dc}=-0.5$ mA, and Fig. 2(d) shows the free layer α as a function of I_{dc} . As before, we observe a linear trend in α as we step I_{dc} . At $I_{dc}=0$, we find $\alpha=0.010\pm 0.002$. The maximum precession angle in these data is $\sim 6.5^\circ$ at $I_{dc}=-0.7$ mA.

As noted above, for each device, we also see a resonant feature that we identify as a fixed-layer dominated mode occurring at a different frequency that is consistent with its estimated anisotropy. The taper and thickness of the fixed layer make quantitative analysis of the damping in these modes difficult, however, as expected¹⁷ for the larger magnetic volume, the linewidth varies only weakly with I_{dc} . In addition, the behavior of this mode shows indications of the dipolar coupling to the free layer, the details of which are presented elsewhere.²⁴

The values of damping that we obtain from the ST-FMR measurements are quite consistent with the results obtained for CoFeB and Py extended thin-film multilayers using either field FMR or time-resolved techniques, 0.006–0.013 for CoFeB (Ref. 25) and 0.006–0.012 for Py.^{11–13} That the ST-FMR measured values of α are on the high end of these ranges can be attributed to the modest enhancement of damping that is expected due to spin pumping^{4,5,12} given the proximity of the Pt capping layer separated from the free layer by 20 nm (5 nm) of Cu in the Py (CoFeB) sample.

Since the values of α determined by the ST-FMR are in accord with standard thin-film FMR measurements, they are much less than the effective damping parameters 0.030–0.035 previously obtained from RT fits using the macrospin approximation to data from short-pulse ST-driven magnetic switching,⁹ which demonstrates the limitations of the macrospin approximation for quantitatively describing large amplitude nanomagnetic dynamics. Micromagnetic modeling, for example, has suggested that magnetic reversal involves multiple, spatially nonuniform modes,^{1,26,27} and in some instances this modeling indicates that such modes can actually enhance spin efficiency in the short-pulse regime.²⁸ Therefore, although macrospin modeling is a useful tool for understanding the critical currents and trends in ST excited dynamics, its predictions are not always numerically definitive with regard to large amplitude ST driven nanomagnet dynamics and switching.

In summary, we have presented ST-FMR measurements of magnetic damping for small-angle magnetic precession in spin valve nanopillars. For devices with CoFeB magnetic layers, we find $\alpha=0.014\pm 0.003$ and for Py, we find $\alpha=0.010\pm 0.002$. These values are consistent with measurements made on continuous films, which demonstrates that processes for fabricating nanoscale structures do not necessarily lead to increased damping at room temperature.

This research was supported in part by the NSF/NSEC program through the Cornell Center for Nanoscale Systems and by the Office of Naval Research. Additional support was provided by NSF through use of the Cornell Nanoscale Science and Technology Facility/NNIN and the facilities of the Cornell Center for Materials Research.

- ¹R. D. McMichael and M. D. Stiles, *J. Appl. Phys.* **97**, 10J901 (2005).
- ²W. J. Gallagher and S. S. S. P. Parkin, *IBM J. Res. Dev.* **50**, 5 (2005).
- ³N. Smith, *J. Appl. Phys.* **99**, 08Q703 (2006).
- ⁴R. Urban, G. Woltersdorf, and B. Heinrich, *Phys. Rev. Lett.* **87**, 217204 (2001).
- ⁵Y. Tserkovnyak, A. Brataas, and G. E. W. Bauer, *Phys. Rev. B* **67**, 140404(R) (2003).
- ⁶Y. Tserkovnyak, A. Brataas, and G. E. W. Bauer, *Phys. Rev. Lett.* **88**, 117601 (2002).
- ⁷I. N. Krivorotov, N. C. Emley, J. C. Sankey, S. I. Kiselev, D. C. Ralph, and R. A. Buhrman, *Science* **307**, 228 (2005).
- ⁸R. H. Koch, J. A. Katine, and J. Z. Sun, *Phys. Rev. Lett.* **92**, 088302 (2004).
- ⁹P. M. Braganca, I. N. Krivorotov, O. Ozatay, A. G. F. Garcia, N. C. Emley, J. C. Sankey, D. C. Ralph, and R. A. Buhrman, *Appl. Phys. Lett.* **87**, 112507 (2005).
- ¹⁰N. C. Emley, I. N. Krivorotov, O. Ozatay, A. G. F. Garcia, J. C. Sankey, and R. A. Buhrman, *Phys. Rev. Lett.* **96**, 247204 (2006).
- ¹¹S. Ingarsson, L. Ritchie, X. Y. Liu, Gang Xiao, J. C. Slonczewski, P. L. Touilloud, and R. H. Koch, *Phys. Rev. B* **66**, 214416 (2002).
- ¹²S. Mizukami, Y. Ando, and T. Miyazaki, *Phys. Rev. B* **66**, 104413 (2002).
- ¹³W. Bailey, P. Kabos, F. Mancoff, and S. Russek, *IEEE Trans. Magn.* **37**, 1749 (2001).
- ¹⁴S. Kaka, M. R. Pufall, W. H. Rippard, T. J. Silva, S. E. Russek, J. A. Katine, and M. Carey, *J. Magn. Magn. Mater.* **286**, 375 (2005).
- ¹⁵M. L. Schneider, M. R. Pufall, W. H. Rippard, S. E. Russek, and J. A. Katine, *Appl. Phys. Lett.* **90**, 092504 (2007).
- ¹⁶A. A. Talapurkar, Y. Suzuki, A. Fukushima, H. Kubota, H. Maehara, K. Tsunekawa, D. D. Kjayaprawira, N. Watanabe, and S. Yuasa, *Nature (London)* **438**, 339 (2005).
- ¹⁷J. C. Sankey, P. M. Braganca, A. G. F. Garcia, I. N. Krivorotov, R. A. Buhrman, and D. C. Ralph, *Phys. Rev. Lett.* **96**, 227601 (2006).
- ¹⁸J. N. Kupferschmidt, S. Adam, and P. W. Brouwer, *Phys. Rev. B* **74**, 134416 (2006).
- ¹⁹A. A. Kovalev, G. E. W. Bauer, and A. Brataas, *Phys. Rev. B* **75**, 014430 (2007).
- ²⁰S. Yuasa, Y. Suzuki, T. Katayama, and K. Ando, *Appl. Phys. Lett.* **87**, 242503 (2005).
- ²¹The thickness of the fixed layers in these samples also makes them sensitive to the taper in the nanopillar sidewalls, which tends to reduce their anisotropy from an ideal value.
- ²²M. Beleggia, M. De Graef, Y. T. Millev, D. A. Goode, and G. Rowlands, *J. Phys. D* **38**, 3333 (2005).
- ²³R. H. Koch, J. A. Katine, and J. Z. Sun, *Phys. Rev. Lett.* **92**, 088302 (2004).
- ²⁴G. D. Fuchs, Ph.D. Thesis, Cornell University, 2007.
- ²⁵C. Bilzer, T. Devolder, J.-V. Kim, G. Counil, C. Chappert, S. Cardoso, and P. P. Freitas, *J. Appl. Phys.* **100**, 053903 (2006). We note that this is not an identical composition of CoFeB.
- ²⁶K.-J. Lee, A. Deac, O. Rendon, J.-P. Nozieres, and B. Dieny, *Nat. Mater.* **3**, 887 (2004).
- ²⁷I. N. Krivorotov, D. V. Berkov, N. L. Gorn, N. C. Emley, J. C. Sankey, D. C. Ralph, and R. A. Buhrman, *Phys. Rev. B* **76**, 024418 (2007).
- ²⁸P. M. Braganca (unpublished).